Acta Crystallographica Section F
Structural Biology and Crystallization Communications
ISSN 1744-3091

Purification, crystallization and preliminary X-ray analysis of truncated and mutant forms of VP4 protease from infectious pancreatic necrosis virus

Jaeyong Lee,[a] Anat R. Feldman,[a] Elaine Chiu,[a] Charlena Chan,[a] You-Na Kim,[a] Bernard Delmas[b] and Mark Paetzel[a]*

[a]Department of Molecular Biology and Biochemistry, Simon Fraser University, South Science Building, 8888 University Drive, Burnaby, British Columbia V5A 1S6, Canada, and [b]Unité de Virologie et Immunologie Moléculaires, Institut National de la Recherche Agronomique, F-78350 Jouy-en-Josas, France

Correspondence e-mail: mpaetzel@sfu.ca

Received 5 September 2006
Accepted 1 November 2006

In viruses belonging to the *Birnaviridae* family, virus protein 4 (VP4) is the viral protease responsible for the proteolytic maturation of the polyprotein encoding the major capsid proteins (VP2 and VP3). Infectious pancreatic necrosis virus (IPNV), the prototype of the aquabirnavirus genus, is the causative agent of a contagious disease in fish which has a large economic impact on aquaculture. IPNV VP4 is a 226-residue (24.0 kDa) serine protease that utilizes a Ser/Lys catalytic dyad mechanism (Ser633 and Lys674). Several truncated and mutant forms of VP4 were expressed in a recombinant expression system, purified and screened for crystallization. Two different crystal forms diffract beyond 2.4 Å resolution. A triclinic crystal derived from one mutant construct has unit-cell parameters a = 41.7, b = 69.6, c = 191.6 Å, α = 93.0, β = 95.1, γ = 97.7°. A hexagonal crystal with space group $P6_122/P6_522$ derived from another mutant construct has unit-cell parameters a = 77.4, b = 77.4, c = 136.9 Å.

1. Introduction

Infectious pancreatic necrosis virus (IPNV) is a well known pathogen in salmonid fish and is responsible for infectious pancreatic necrosis (IPN), a disease characterized by severe damage to the internal organs and tissues (Roberts & Pearson, 2005). Owing to the high mortality rate and its widespread distribution, this virus is a major economical and ecological threat to the aquaculture and sea-farming industry worldwide (Reno, 1999).

IPNV belongs to the genus *Aquabirnavirus* in the virus family *Birnaviridae* (Dobos, 1995). This virus family is characterized by a bi-segmented double-stranded RNA genome encapsulated in a non-enveloped icosahedral virion that is approximately 60 nm in diameter (Delmas *et al.*, 2005; http://www.ncbi.nlm.nih.gov/ICTVdb/Ictv/index.htm). The larger genomic segment (segment A) encodes a polyprotein (NH_2-pVP2-VP4-VP3-COOH) that contains precursors to the major capsid proteins pVP2 and VP3. These two proteins are released by the proteolytic activity of VP4 (virus protein 4), a serine protease that utilizes a Ser/Lys catalytic dyad mechanism (Birghan *et al.*, 2000; Lejal *et al.*, 2000; Petit *et al.*, 2000). VP4 is also believed to be responsible for the further maturation of pVP2 to generate VP2 and additional peptides that are also found in the mature virion (Da Costa *et al.*, 2002, 2003; Galloux *et al.*, 2004). The VP4 proteolytic activity appears to be closely coupled to the virus life cycle and particularly to capsid assembly.

The structure of a VP4 protease from another member of the *Birnaviridae*, blotched snakehead virus (BSNV), has previously been described (Feldman *et al.*, 2006). Despite having a very low level of sequence similarity, it reveals an active site with structural similarities to other characterized Ser/Lys proteases such as bacterial signal peptidase (Paetzel *et al.*, 1998, 2002, 2004), LexA protease (Luo *et al.*, 2001) and Lon proteases (Botos *et al.*, 2004, 2005; Im *et al.*, 2004).

While the essential catalytic residues are conserved between the VP4 proteases in BSNV and IPNV [Ser633/Lys674 for IPNV VP4 (Petit *et al.*, 2000); Ser692/Lys729 for BSNV VP4 (Da Costa *et al.* 2003)], there is very little overall primary sequence identity (~19%) between these enzymes (Da Costa *et al.*, 2003). The difference also extends to the specificity of the cleavage site as the consensus IPNV

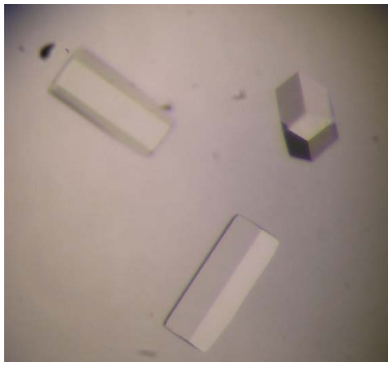

Table 1
The optimized crystallization conditions for the various constructs of IPNV VP4 protease.

Crystal	Form 1	Form 2	Form 3	Form 4	Form 5
VP4 construct	514–734-Hx6	514–715,K674A	514–716,K674A	514–716,K674A	524–716,K674A
Concentration (mg ml^{-1})	30	48	58	59	30
Temperature (K)	277	298	277	277	291
Crystallization conditions	0.1 *M* Tris pH 8.5, 20% PEG 2K MME, 2 *M* NaCl	0.1 *M* Na citrate pH 5.6, 1.0 *M* $(NH_4)H_2PO_4$, 3%(*w*/*v*) D-(+)-sucrose	0.1 *M* MES pH 6.0, 20% PEG 2K MME, 3 *M* NaCl	0.1 *M* Tris pH 8.5, 31% PEG 4K, 0.4 *M* Li_2SO_4, 0.2 *M* guanidine–HCl	0.1 *M* Tris pH 8.5, 17% PEG 3350, 0.4 *M* Ca acetate
Maturation time (weeks)	3–4	2–3	3–4	1–2	1–2
Cryoconditions	0.1 *M* Tris pH 8.5, 20% PEG 2K MME, 2 *M* NaCl, 10% glycerol	0.1 *M* Na citrate pH 5.6, 1.0 *M* $(NH_4)H_2PO_4$, 30% glycerol	0.1 *M* MES pH 6.0, 30% PEG 2K MME, 1.2 *M* NaCl	0.1 *M* Tris pH 8.5, 35% PEG 4K, 0.45 *M* guanidine–HCl, 10% glycerol	0.1 *M* Tris pH 8.5, 20% PEG 3350, 0.4 *M* Ca acetate, 10% glycerol
Diffraction	Anisotropic (~3.0 Å)	Anisotropic (~4.0 Å)	Anisotropic (~3.5 Å)	Beyond 2.4 Å (see Table 2)	Beyond 2.4 Å (see Table 2)

polyprotein cleavage motif is defined by (Ser/Thr)-*X*-Ala↓(Ser/Ala)-Gly, whereas in BSNV it is defined by Pro-*X*-Ala↓(Ala/Ser).

The IPNV polyprotein (NH_2-pVP2-VP4-VP3-COOH) encoded by the segment A gene (~3100 bp) is 972 residues in length (Dobos, 1995). The primary VP4 cleavage sites (scissile bond) at the pVP2–VP4 and VP4–VP3 junctions are located between residues 508/509 and 734/735. These cleavage sites define the length of the IPNV VP4 protease as 226 residues (24.0 kDa), starting at Ser509 and ending at Ala734 in the polyprotein. In addition to these primary cleavage junctions, a subsidiary cleavage site within the VP4 polypeptide sequence also exists between residues Arg715 and Ala716 (Petit *et al.*, 2000).

During overexpression of recombinant IPNV VP4 in *Escherichia coli*, we observed a self-cleavage activity which could be blocked by introducing an active-site mutation (Lys674 to Ala). Interestingly, the self-truncated version of the wild-type VP4 appeared to be a better crystallization candidate than the full-length VP4. Thereafter, we created various active-site mutant constructs of IPNV VP4 with different truncations at the N- and C-termini and the purified proteins were screened for crystallization. In this report, we present the crystallization and preliminary diffraction analysis of various IPNV VP4 constructs. Two IPNV VP4 constructs produced well diffracting crystals suitable for structure solution.

2. Materials and methods

2.1. Site-directed mutagenesis and cloning

All site-directed mutagenesis was carried out using the QuikChange kit (Stratagene) and the insert sequences in all plasmid constructs were verified by DNA sequencing. The parental template plasmid used in this study was pET-28b-IPNV_VP4(514–734-Hx6), which has a VP4 gene insert (cloned into the *Nco*I/*Xho*I cloning sites) with a wild-type active site. This construct encodes polyprotein residues Gly514–Ala734, followed by a plasmid-encoded 6×His tag at the C-terminus. To inactivate the protease, the active-site residue Lys674 was converted to Ala. The plasmid pET-28b-IPNV_VP4(514–734-Hx6) was used as the template and the forward primer 5′-CAA TCT GCG GTG TAG ACA TCG CAG CCA TCG CAG CCC ACG AAC-3′ and the reverse primer 5′-GTT CGT GGG CTG CGA TGG CTG CGA TGT CTA CAC CGC AGA TT-3′ were used for the mutagenesis reaction. The resulting plasmid was termed pET-28b-IPNV_VP4(514–734,K674A-Hx6) and was used for generating the C-terminal truncation constructs.

A mutant construct ending with Arg715 was generated by converting the codon encoding Ala716 to a stop codon using the forward primer 5′-CCC TGC CCG TAC AAC GCT AAA AGG GCT CCA ACA AGA G-3′ and the reverse primer 5′-CTC TTG TTG GAG CCC TTT TAG CGT TGT ACG GGC AGG G-3′. The resulting plasmid was termed pET-28b-IPNV_VP4(514–715,K674A). Another mutant construct ending with Ala716 was generated by converting the codon encoding Lys717 to a stop codon using the forward primer 5′-CTG CCC GTA CAA CGC GCA TAA GGC TCC AAC AAG AGG ATC-3′ and the reverse primer 5′-GAT CCT CTT GTT GGA GCC TTA TGC GCG TTG TAC GGG CAG-3′. The resulting plasmid was termed pET-28b-IPNV_VP4(514–716,K674A).

In order to generate the N-terminal truncation mutant that starts at residue Lys524, pET-28b-IPNV_VP4(514–716,K674A) was used as the template in the PCR reaction. The DNA insert fragment encoding residues Lys524–Ala716 with an active-site mutation (K674A) was amplified using the forward primer 5′-CAT ATG CTG GAG TCC GCC AAC TAC GAG GAA GTC-3′ and the reverse primer 5′-GTC GAC TCA TGC ATT TGA TGC CAT CAG CTC TCC CAG G-3′ and was cloned into pET-24a+ (Novagen) *via* the *Nde*I and *Sal*I restriction sites. The resulting plasmid was termed pET-24a-IPNV_VP4 (524–716,K674A).

2.2. Protein overexpression and purification

All plasmid constructs were transformed into *E. coli* strain Tuner (DE3) and selected on LB agar plates containing kanamycin (0.05 mg ml^{-1}). A single transformant colony was used to inoculate a 100 ml overnight culture at 310 K with shaking. A 10 ml aliquot of the overnight culture was then used to inoculate 1 l fresh LB supplemented with kanamycin (0.05 mg ml^{-1}). The cells were grown for approximately 4 h at 310 K with shaking (250 rev min^{-1}) and were then induced with IPTG (0.5 m*M* final concentration). After 3 h induction, the cells were harvested by centrifugation at 5000*g* for 15 min. The cell pellets were frozen at 193 K.

The cells were lysed by completely resuspending the frozen cell pellet (4 g) in 30 ml lysis buffer (50 m*M* Tris–HCl pH 8.0, 10% glycerol, 1 m*M* DTT, 7 m*M* magnesium acetate, 0.2 mg ml^{-1} lysozyme, 1 U ml^{-1} benzonase and 0.1% Triton X-100) and then incubating overnight with gentle shaking at 277 K. The cell lysate was spun at 27 000*g* for 30 min to obtain the soluble fraction. The overexpression of VP4 constructs were confirmed by SDS–PAGE and Coomassie staining and all protein fractions resulting from subsequent purification steps were analyzed by the same method.

The soluble fraction was subjected to ammonium sulfate fractionation using 30, 40, 50 and 60%(*w*/*v*) ammonium sulfate concentrations. The fractionated pellets were redissolved in a minimal volume of buffer *A* (20 m*M* Tris–HCl pH 8.0, 10% glycerol, 1 m*M* EDTA, 50 m*M* NaCl, 1 m*M* DTT). The fractions containing the protein were dialyzed overnight in buffer *A* and then applied onto a Q-Sepharose FF anion-exchange column (2 ml bed volume) equilibrated in the same buffer. The column was washed with 10 ml buffer

Table 2
Data-collection statistics for crystals derived from two IPNV VP4 mutant constructs: form 4, VP4 (514–716,K674A), and form 5, VP4 (524–716,K674A).

Crystal	Form 4	Form 5
Crystal-to-detector distance (mm)	200	200
Oscillation angle (°)	0.5	0.5
No. of images	720	198
Exposure time (min)	2	2
Wavelength (Å)	1.5418	1.5418
Temperature (K)	100	100
Space group	*P*1	$P6_122/P6_522$
Unit-cell parameters		
a (Å)	41.7	77.4
b (Å)	69.6	77.4
c (Å)	191.6	136.9
α (°)	93.0	90
β (°)	95.1	90
γ (°)	97.7	120
Resolution range (Å)	54.1–2.4 (2.5–2.4)	32.6–2.4 (2.5–2.4)
Total no. of reflections	250114	106566
No. of unique reflections	71206	9408
Average redundancy	3.5 (3.5)	11.3 (11.8)
Completeness (%)	90.2 (83.7)	98.2 (97.2)
$R_{\rm merge}$†	0.037 (0.096)	0.112 (0.387)
$\langle I/\sigma(I)\rangle$	20.9 (9.7)	15.1 (6.5)

† $R_{\rm merge} = \sum_{hkl}\sum_j |I_j(hkl) - \langle I(hkl)\rangle| / \sum_{hkl}\sum_j \langle I(hkl)\rangle$, where $I_j(hkl)$ and $\langle I(hkl)\rangle$ are the intensity of measurement *j* and the mean intensity for the reflection with indices *hkl*, respectively.

A and eluted *via* a step gradient with 3 ml aliquots of buffer *A* at 0.1, 0.2, 0.3, 0.35, 0.4, 0.5 and 1.0 *M* NaCl concentrations. The fractions containing the protein were pooled and concentrated and subjected to gel filtration (AKTA Prime system, Pharmacia). The gel-filtration column (HiPrep 16/60 Sephacryl S-100 HR) was pre-equilibrated in buffer *B* [20 m*M* Tris–HCl pH 8.0, 10% glycerol, 100 m*M* NaCl, 1%(*v*/*v*) β-mercaptoethanol]. The mobile phase was run at a 1 ml min^{-1} flow rate and the elution was collected in 3 ml fractions. All VP4 mutant constructs eluted from the gel-filtration column in a manner consistent with them being monomeric in solution. The fractions containing the purified protein were pooled and concentrated by centrifugal filtration (5 kDa cutoff; Millipore) for crystallization. The protein concentration was determined by measuring UV absorption at 280 nm. The extinction coefficient that was used for all protein constructs (9970 M^{-1} cm^{-1}) was calculated using the *ProtParam* tool server (http://ca.expasy.org/tools/protparam.html).

2.3. Crystallization

The purified proteins were initially screened for crystallization using Crystal Screens 1 and 2 (Jancarik & Kim, 1991) and PEG/Ion Screen from Hampton Research. The crystal screens were carried out at both 277 K and room temperature and were conducted either by hanging-drop or sitting-drop vapour diffusion. The crystallization drops were made by mixing 1 µl protein sample with 1 µl reservoir solution and then equilibrated over 1 ml reservoir solution. For optimization, sitting drops over a 1 ml reservoir volume were used. Grid screens based on the initial hits were used to optimize the protein concentration, precipitant concentration, pH and additives. The final optimized conditions are listed in Table 1.

2.4. X-ray diffraction analysis

The crystals were transferred by pipette to the cryosolution and soaked for approximately 5 min (for cryosolutions, refer to Table 1). The crystals were looped out of the cryosolvent with a copper mounted loop (Hampton Research) and immediately placed on a goniometer in the path of a nitrogen-gas stream (X-stream2000 cryosystem set at 100 K). The diffraction data were collected using an MSC Rigaku X-ray diffraction analysis system. The X-ray generator was a MicroMax-007 with a Cu anode operating at 40 kV and 20 mA. The X-ray beam was focused with Osmic Confocal VariMax High Flux optics and the reflections were recorded using an R-AXIS IV^{++} image plate. The data collection, indexing, integration and scaling were carried out using the program *CrystalClear* (Pflugrath, 1999). The data-processing statistics are shown in Table 2.

3. Results and discussion

The VP4(514–734-Hx6) construct, with a wild-type active site, undergoes an efficient self-cleavage reaction when overexpressed in *E. coli*. The cleavage results in a smaller truncated version of VP4 without the His tag at the C-terminus. An active-site mutant construct, VP4(514–734,K674A-Hx6), with Lys674 mutated to an alanine, was thus designed to prevent this self-cleavage activity. When initial crystallization screening was conducted with these two forms of VP4, only the cleaved form originating from the wild-type VP4(514–734-Hx6) construct yielded crystallization hits. Under an optimized condition (Table 2; form 1), this form of VP4 nucleates in 3–4 d as tiny needles that eventually mature into long and often split needles over a period of three weeks (form 1; Fig. 1*a*). However, X-ray diffraction analysis of this crystal form resulted in low resolution and anisotropic data.

The apparent self-cleavage activity of VP4 was likely to take place at an internal cleavage site as described in an earlier study (Petit *et al.*, 2000). Since this subsidiary cleavage was reported to occur between Arg715 and Ala716 (which interestingly does not match the consensus cleavage sequence), we engineered stop codons at positions 716 and 717 in VP4(514–734,K674A-Hx6) to generate the

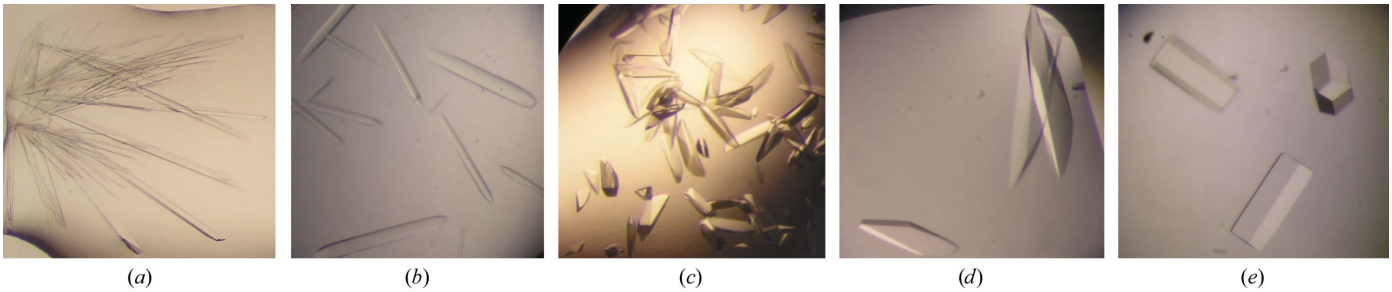

(*a*) (*b*) (*c*) (*d*) (*e*)

Figure 1
The crystals obtained from the various constructs of IPNV VP4 protease. (*a*) Form 1 (0.05 × 0.1 × 1.0 mm) derived from the self-cleavage product originating from the construct 514–734-Hx6; (*b*) form 2 (0.05 × 0.1 × 0.8 mm) derived from the construct 514–715,K674A; (*c*) form 3 (0.1 × 0.1 × 0.3) derived from the construct 514–716,K674A; (*d*) form 4 (0.1 × 0.2 × 0.4 mm) also derived from the construct 514–716,K674A; (*e*) form 5 (0.1 × 0.1 × 0.3 mm) derived from the construct 524–716,K674A.

constructs VP4(514–715,K674A) and VP4(514–716,K674A), respectively. Both constructs yielded multiple hits during initial crystallization screening and these conditions were optimized for crystal growth. The VP4(514–715,K674A) construct (203 residues, 21.6 kDa) crystallized under similar conditions to that of the self-cleaved form of VP4. A novel hit condition at room temperature, when optimized (Table 1; form 2), produced sizeable needle-shaped crystals (form 2; Fig. 1*b*). However, the diffraction was anisotropic and limited to relatively low resolution. On the other hand, the VP4(514–716, K674A) construct (204 residues, 21.7 kDa) yielded two distinct optimized crystallization conditions at 277 K (Table 1; forms 3 and 4). While form 3 (Fig. 1*c*) displayed an anisotropic diffraction pattern of low resolution, form 4 (Fig. 1*d*), with average dimensions of 0.1 × 0.2 × 0.4 mm, gave relatively high-quality diffraction (for diffraction statistics, see Table 2). Diffraction analysis and a rotation-function calculation using *MOLREP* (Vagin & Teplyakov, 1997) from the *CCP*4 suite (Collaborative Computational Project, Number 4, 1994) are consistent with this crystal form being triclinic. Calculation of the Matthews coefficient (Kantardjieff & Rupp, 2003; http://www.ruppweb.org/mattprob/) suggests that the most plausible number of molecules in the asymmetric unit is nine to 11 monomers, with respective solvent contents of 56.1, 51.3 and 46.4%. Their corresponding Matthews coefficient values are 2.8, 2.5 and 2.3 Å^3 Da^{-1}, respectively.

The C-terminal truncations of VP4 may aid crystallization by removing a flexible region that is presumably required for efficient substrate presentation during the polyprotein processing. Since VP4 is encoded in the central domain of the polyprotein and the cleavage occurs at both its N- and C-terminus, a flexible region may also exist at the N-terminus of VP4. We reasoned that its removal might improve the quality of the crystals. Therefore, an additional protein construct VP4(524–716,K674A) was engineered with ten additional residues removed from the N-terminus. After the initial methionine, the expressed protein starts at Leu524 and ended with Ala716 (194 residues; 20.5 kDa). When the initial crystallization condition was optimized (Table 1; form 5), this construct formed hexagon-shaped crystals (Fig. 1*e*) with average dimensions of 0.1 × 0.1 × 0.3 mm (maximum dimensions 0.3 × 0.3 × 0.5 mm). Initial diffraction analysis of this crystal form shows diffraction beyond 2.4 Å resolution (Table 2; form 5) and is consistent with the crystal belonging to space group $P6_122$ or $P6_522$, with one molecule in the asymmetric unit (V_M of 2.9 Å^3 Da^{-1} and 57.3% solvent content; http://www.ruppweb.org/mattprob/).

This work was supported in part by a Canadian Institute of Health Research operating grant (to MP), a National Science and Engineering Research Council of Canada discovery grant (to MP), a Michael Smith Foundation for Health Research Scholar award (to MP), a Canadian Foundation of Innovation grant (to MP) and a Canadian Cystic Fibrosis Foundation Postdoctoral Fellowship Award (to AF). BD acknowledges support from the ACI 'Microbiologie' of the French MRT.

References

Birghan, C., Mundt, E. & Gorbalenya, A. E. (2000). *EMBO J.* **19**, 114–123.
Botos, I., Melnikov, E. E., Cherry, S., Kozlov, S., Makhovskaya, O. V., Tropea, J. E., Gustchina, A., Rotanova, T. V. & Wlodawer, A. (2005). *J. Mol. Biol.* **351**, 144–157.
Botos, I., Melnikov, E. E., Cherry, S., Tropea, J. E., Khalatova, A. G., Rasulova, F., Dauter, Z., Maurizi, M. R., Rotanova, T. V., Wlodawer, A. & Gustchina, A. (2004). *J. Biol. Chem.* **279**, 8140–8148.
Collaborative Computational Project, Number 4 (1994). *Acta Cryst.* D**50**, 760–763.
Da Costa, B., Chevalier, C., Henry, C., Huet, J.-C., Petit, S., Lepault, J., Boot, H. & Delmas, B. (2002). *J. Virol.* **76**, 2393–2402.
Da Costa, B., Soignier, S., Chevalier, C., Henry, C., Thory, C., Huet, J.-C. & Delmas, B. (2003). *J. Virol.* **77**, 719–25.
Delmas, B., Kibenge, F. S. B., Leong, J. C., Mundt, E., Vakharia, V. N. & Wu, J. L. (2005). *Virus Taxonomy: The Eighth Report of the International Committee on Taxonomy of Viruses*, edited by C. M. Fauquet, M. A. Mayo, J. Maniloff, U. Desselberger & L. A. Ball, pp. 561–569. Amsterdam: Elsevier.
Dobos, P. (1995). *Annu. Rev. Fish Dis.* **5**, 25–54.
Feldman, R. A., Lee, J., Delmas, B. & Paetzel, M. (2006). *J. Mol. Biol.* **358**, 1378–1389.
Galloux, M., Chevalier, C., Henry, C., Huet, J.-C., Da Costa, B. & Delmas, B. (2004). *J. Gen. Virol.* **85**, 2231–2236.
Im, Y. J., Na, Y., Kang, G. B., Rho, S. H., Kim, M. K., Lee, J. H., Chung, C. H. & Eom, S. H. (2004). *J. Biol. Chem.* **279**, 53451–53457.
Jancarik, J. & Kim, S.-H. (1991). *J. Appl. Cryst.* **24**, 409–411.
Kantardjieff, K. & Rupp, B. (2003). *Protein Sci.* **12**, 1865–1871.
Lejal, N., Da Costa, B., Huet, J. C. & Delmas, B. (2000). *J. Gen. Virol.* **81**, 983–992.
Luo, Y., Pfuetzner, R. A., Mosimann, S., Paetzel, M., Frey, E. A., Cherney, M., Kim, B., Little, J. W. & Strynadka, N. C. (2001). *Cell*, **106**, 585–594.
Paetzel, M., Dalbey, R. E. & Strynadka, N. C. (1998). *Nature (London)*, **396**, 186–190.
Paetzel, M., Dalbey, R. E. & Strynadka, N. C. (2002). *J. Biol. Chem.* **277**, 9512–9519.
Paetzel, M., Goodall, J. J., Kania, M., Dalbey, R. E. & Page, M. G. (2004). *J. Biol. Chem.* **279**, 30781–30790.
Petit, S., Lejal, N., Huet, J.-C. & Delmas, B. (2000). *J. Virol.* **74**, 2057–2066.
Pflugrath, J. W. (1999). *Acta Cryst.* D**55**, 1718–1725.
Reno, P. (1999). *Fish Diseases and Disorders*, Vol. 3, edited by P. T. K. Woo & D. W. Bruno, pp. 1–55. New York: CABI.
Roberts, R. J. & Pearson, M. D. (2005). *J. Fish Dis.* **28**, 383–390.
Vagin, A. & Teplyakov, A. (1997). *J. Appl. Cryst.* **30**, 1022–1025.